Islamic Azad University
Mashhad Branch

Geochemical and Sedimentary Changes of the Mighan Playa in Arak, Iran

Feridon Ghadimi* **and Mohammad Ghomi**

Department of Mining Engineering, Arak University of Technology, PO BOX 38181-41167, Arak, Iran

Received 23 June 2012; accepted 12 January 2013

Abstract

The Mighan Playa is the largest playa in Markazi Province. Sedimentary and soil structures show that during all phases the playa was ephemeral. The duration and frequency of flooding varied causing variations in the relative amounts of accumulation, and soil formation. The clastic fraction of the playa sediment consists of quartz, mica and chlorite while the non-clastic evaporite fraction is dominated by gypsum, calcite, glauberite, thenardite and halite. Using the principle of chemical divides, such variations in mineralogy have been explained in terms of a change in brine chemistry from Na-Ca-Mg-SO_4-Cl to Na-SO_4-Cl type. It is also suggested that at an earlier stage, Mighan playa brine underwent evaporation under the conditions of Ca>alkalinity whereas in more recent times, the evaporite mineralogy has developed with alkalinity>Ca. The shallow depth cores are divided into distinct geochemical units based on elemental ratios. Units I and III reflect high chemical weathering whereas the middle unit, II, indicates relatively low weathering and enrichment in evaporites.

Keywords: *Mighan Playa, Sedimentary Facies, Evaporites, Geochemical Unit.*

1. Introduction

The geochemical evolution of a playa is governed primarily by the inflow composition, selective removal of solutes and evaporative concentrations. The formation of evaporite mineral is dictated by the concept of chemical divides [2]. The stratigraphic variation in the mineralogy of playa sediments is also an indicator of past salinity conditions and hydrological changes. Such variations have been extensively used to deduce Quaternary paleoclimatic fluctuations in many parts of the world [6, 7, 12]. Different evaporite mineral assemblages can reflect the chemical weathering of different rocks, the mixing of inflow waters from several sources, and various hydrochemical and physical processes. Study of evaporite mineral assemblages is increasingly being used to detect saline phases during the reconstruction of a paleoenvironment [8, 10].

The water budget of the closed basin playas is sensitive to climate changes. Sediments deposited in these closed basins are influenced by both the quality (salinity, composition) and quantity (influx of detrital) of the inflows. Depending upon the salinity and composition of the brine, a number of authigenic minerals (evaporite) precipitated. Accordingly, evaporites are deposited during arid phases and detritals are transported into the playa during humid periods.

In the last couple of years, a number of attempts have been made to understand the paleohydrology from the overall mineralogy and inorganic composition of the sediments [4, 8, 12, 20].

This work attempts to compare the sedimentology, mineralogy and geochemistry of the late Holocene sediments of the Mighan playa in order to understand the sedimentology and the geochemical history of the playa with implications for late climatic fluctuations.

2. Regional Setting

The Mighan playa is bounded to the south and north by the high Arak and Ashtian, Mountains of Mesozoic and Cenozoic age. These mountains also divide the region into a mountainous part and semi-arid central portion (Mighan playa). The Mighan playa has an annual rainfall of 150-350 mm with an average annual temperature of 19^{o} C. The basement of the playa is made up of Cretaceous limestone. The total catchment area of the playa is 5500 Km^2. The playa occupies an area of about 110 Km^2 . The average water depth is approximately 0.5 m with a maximum depth of about 1 m.

Two major ephemeral streams, namely the Gharakahriz and Ashtian as well as many minor ones from the Farmahin, Amanabad and Haftadgholeh areas feed the playa. The Gharakahriz River near the city of Arak, the largest feeder stream, originates from south of the playa while the Ashtian River rises from the city of Ashtian and flows toward the south where it enters

---

*Corresponding author.
E-mail address (es): drghadimi@yahoo.com

the playa. In spite of a large catchment area, the Mighan playa presently receives very little runoff due to present climatic conditions. The surface of the Mighan playa presently undergoes complete desiccation every summer forming an efflorescent crust. This crust essentially consists of gypsum, glauberite, halite and calcite [21]. It dissolves when it comes in contact with fresh run off during the next rain and this process increases the solute load of the playa brine. In terms of chemical composition, the brine is known to be particularly high in Ca and Na [11]. Na_2SO_4, NaCl and $CaSO_4$ are the main constituents of the brine.

This playa receives sediments from the weathering of the highly folded and metamorphosed Mesozoic rocks of the Arak Mountains in the south and sedimentary, volcanic rocks of the Ashtian Mountains in the north. The mountains of Arak are comprised of slate, phyllite and crystallized limestone while the mountains of Ashtian include limestone, sandstone, tuff, shale and lava [1] (Fig. 1). According to Pedrami[13] the sedimentation rate in the Mighan playa is 2.5 m per 1000 years. The thickness of the sediments in the Mighan playa is 140 m and is Pre-Holocene.

3. Methods

Sediment samples from several locations along the depth profiles were collected from the Mighan playa. The locations of the sampling points were fixed with a GPS and are shown on the location map (Fig. 1). Sediments from cores (up to 10 m) were collected from four augured holes of the Mighan playa at interval of 1.5 to 2 m. Samples for mineralogical and geochemical analysis were subjected to pre-treatments such as air drying at 50^o C, homogenization and grinding to 200 mesh size in an agate mortar mill. The powdered samples were used to identify and quantify the minerals present by X-Ray Diffraction (XRD) and the major as well as trace elements by X-Ray Fluorescence (XRF) analyses. The bulk of the desalted and textured samples were run on a Siemense (D_{500}) diffractometer, using a Cu target.

For trace elements, powdered specimens in plastic cups were analyzed using Cu filters on an XRF instrument. For major elements, glass transformed specimens were prepared by mixing and then heated in platinum crucibles using gas burners for 30 min. The analytical accuracy for the XRF measurements was <5% and precision was <2%.

4. Sediment

4.1. Sediment Within Playa

On the basis of examination of the cores, a facies classification of the playa and related sediments was developed (facies I, II, III and IV in Fig. 2). Facies include (1) gray and red mud facies (facies I, III and IV) and (2) sodium–bearing sulfate facies (facies II).

4.1.1. MUD Facies

Youngest gray mud (facies I)

Plastic wet muds dry and form cracks that are open to a depth of about 1 m. At this depth, curved slickensided fractures related to pedogenic processes are abundant. Woody living and decayed roots extend to a depth of more than 1 m. Sulfate (gypsum), chloride (halite), calcite, chlorite and muscovite are present in sparse amounts.

At a depth of about 1 m below the surface of the playa in the study area, changes in texture and color of the sediment can be observed. At a depth of 1 to 1.4 m, the base of the youngest mud is marked by a decreasing abundance of modern roots, slightly increasing stiffness of the mud, larger and better developed slickenside, planar fractures interpreted as vertical soil structures, and slightly lighter gray colors.

Older, gray mud (facies III)

Gray mud is massive or mottled silty clay with variable amounts of admixed silt. It is fairly plastic near the surface and becomes stiffer at deeper depths. Textures generally resemble those of the youngest mud. A few of the older gray muds have preserved sedimentary structures, including some intervals of fine lamination within the clays and where the clays are inter-bedded with sand and silt. Most gray mud beds are stiff and have been fractured. The fractured surfaces have been mineralized by black iron or hydroxides.

A variety of color modifications of gray mud beds is apparent. Gray colors vary from as dark as the surface soil to light gray, probably reflecting variable preservation of organic material. Many older gray mud beds contain evaporite minerals (gypsum, halite) and clastic minerals (quartz, chlorite, muscovite and talk).

Red muds (facies IV)

Although reddish muds resemble gray muds in texture, appearance, and occurrence, they are colored, red-brown. Red muds, massive or locally laminated, are typically firm, containing a fractured surface pigmented by iron and hydroxides. The colors in muds may indicate either post-depositional oxidation or conditions of less effective reduction in the lake environment.

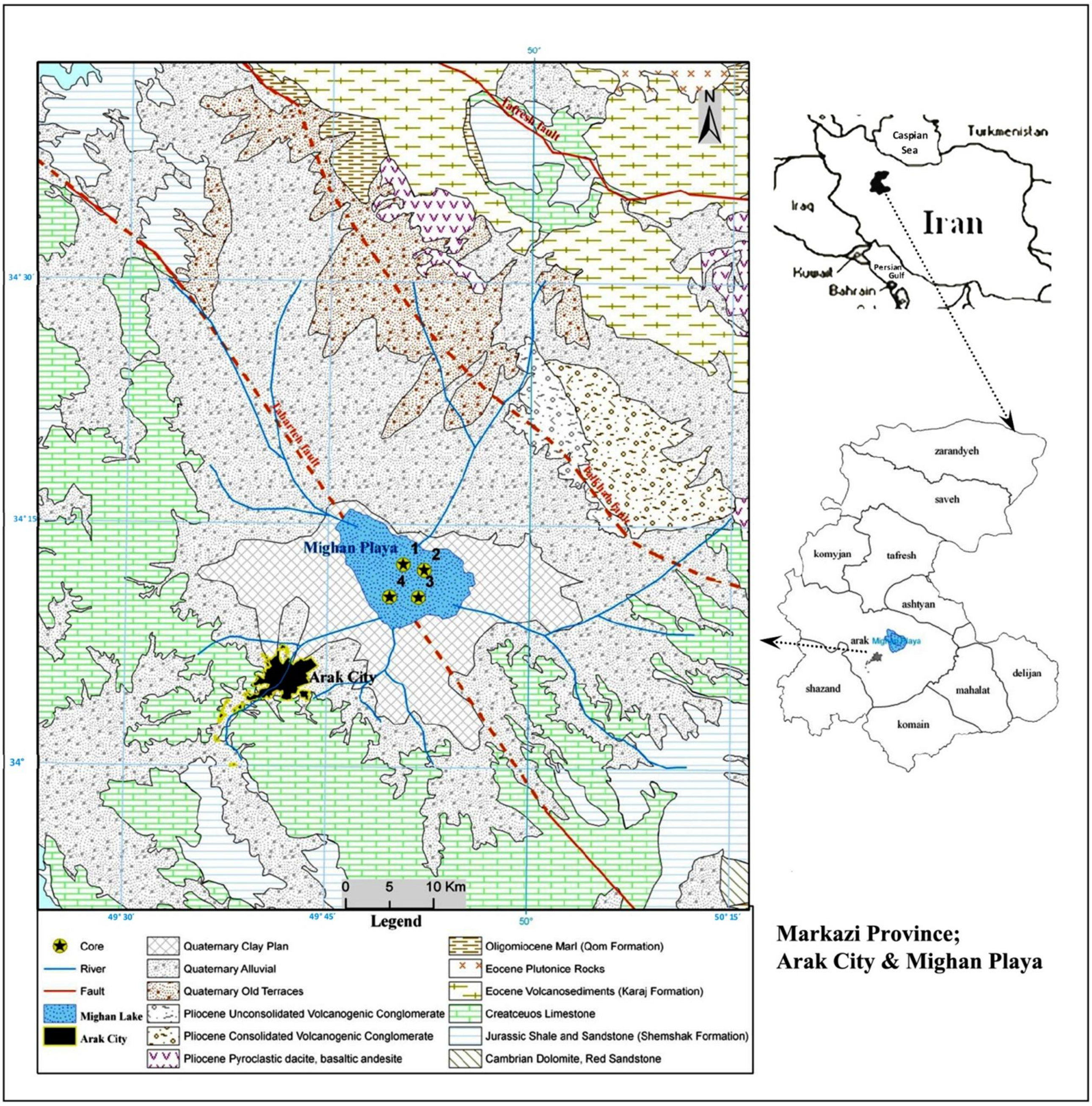

Fig. 1. Location map of the Mighan playa. (The coring points are indicated in playa).

4.2. Sodium-bearing Sulfate Facies (facies II)

The deposits of Mighan Lake (Fig. 2) mainly consist of glauberite rich sediments [$Na_2(SO_4)_2$] that are partly unstratified and partly layered due to variations in clay content and crystal size(facies II). The cores above and below these sulfate beds include some high clay/glauberite. In all parts of the cores with the mentioned salt beds, glauberite is only largely absent from the sediments in the lower 7.5 m of the core where gypsum ($CaSO_4.2H_2O$), halite (NaCl), basanite($2CaSO_4.H_2O$) and calcite ($CaCO_3$) are the dominant salt minerals.

One important textural aspect of the glauberite-rich deposits is the presence or absence of layering, on a millimeter to centimeter scale, due to variations in the relative amounts of clay and glauberite and/or variations in the size of the glauberite crystals. Within the lowest intervals with predominantly unstratified deposits, several sections are characterized both by low glauberite content and by gluaberite crystals of large size (1-5 mm). In the central part of these sections, the deposits are laminated and contain only a few or no glauberite crystals at all. Outside of these central parts, the deposits are not laminated and do not contain any relics of a laminated structure; they also have a higher glauberite content, which often increases away from the center. Some of these transitional unites are characterized by a gradual decrease in crystal size in the same direction.

In all intervals with unstratified deposits, the size of a large portion of the glauberite crystals is greater than 0.5 mm. In the layered intervals, the average size of the crystals is most commonly below that value; this size limit is regularly exceeded, but never throughout several successive layers. Within the layered intervals, the layers with an important admixture of detrital mud are commonly characterized by low glauberite content and a large crystal size (0.5-1 mm).

5. Mineralogy of Playa Sediments

Bulk mineralogy of playa sediment consists of two major groups; (a) the association of clastics and (b) evaporites precipitated from the playa brine (Table 1). Along the depth profiles, the associations of clastics do not show any major differences among the sediment facies. But these facies are quite distinctive in terms of evaporite mineralogy. Data on clastic and evaporite mineralogy in the four sedimentation facies are presented in Table 2. Quartz is present in abundance in the middle and the depth facies whereas muscovite and chlorite are more abundant in the upper and lower facies. Talc is present in facies IV.

The association of evaporite minerals is broadly comparable in the depth facies of the Mighan playa. Facies I is enriched in gypsum while facies II shows a higher abundance of glauberite and thenardite with a depleted gypsum content. Similarly facies III and V are enriched in gypsum, basanite and halite. Calcite and magnesite are minor mineral in these facies.

6. Geochemical Unites

On the basis of the concentration of trace elements and oxides of major elements, the Mighan playa lake is divided into characteristic geochemical unites at the depth cores (I, II, III and IV from surface to depth) (Fig. 3a, 3b). We have used several geochemical ratios such as Na_2O/Al_2O_3, Na_2O/K_2O, Zr/Al_2O_3, SiO_2/K_2O and Sr/Ba to divide the depth cores into three different geochemical unites (i.e. I to III) (Fig. 3a). The ratios Na_2O/Al_2O_3 and Na_2O/TiO_2 represent the ratios of soluble oxides to hydrolysates and indicate the degree of chemical weathering of the detrital fraction [15]. The Na_2O/K_2O ratio also behaves in a similar manner because of the different solution and adsorption behavior of alkalis (e.g. K is largely adsorbed by fine grained material). The ratios Zr/Al_2O_3 and SiO_2/Al_2O_3 indicate terrigenous input in the sediments and the Sr/Ba ratio reflects carbonate to detrital fraction. For two of the cores, the ratios Na_2O/Al_2O_3, Na_2O/K_2O show a very similar trend and the distribution of Zr/Al_2O_3 and SiO_2/Al_2O_3 are also comparable. We selected predominantly geochemical ratios, Na_2O/Al_2O_3, Zr/Al_2O_3 and Sr/Br for characterizing the depth cores of Mighan Lake (Fig. 3a). In general, the uppermost and lowermost units (I and III, respectively) exhibit relatively lower values of Na_2O/Al_2O_3 ratio (and also Na_2O/K_2O) compared to the intermediate unite (II). The Sr/Ba ratio is lowest in unite II and the Zr/Al_2O_3 and SiO_2/Al_2O_3 ratio is highest in unites I and III.

The concentration of trace elements (in mg/kg) and oxides of the major elements (in mass%) presented in Fig. 3 as average values for different unites, are comparable in depth profiles in four cores. Similar to the oxide ratio, we have three unites in four cores. The uppermost and lowermost unites (I and III) exhibit higher CaO and lower SiO_2. For trace elements, the uppermost and lowermost unites are enriched in Sr and lower in Zr (Fig. 3b). In Table 3 average values for major oxides and trace elements are comparable in the depth profiles of all cores.

Table 1. Major evaporite and clastic minerals in Mighan Lake sediments as inferred from X-Ray diffraction patterns.

	Composition
Carbonates	
Calcite	$CaCO_3$
Magnesite	$MgCO_3$
Chloride	
Halite	NaCl
Sulfates	
Gypsum	$CaSO_4.2H_2O$
Basanite	$CaSO_4.1/2H_2O$
Glauberite	$Na_2Ca(SO_4)_2$
Thenardite	Na_2SO_4
Gorgeyite	$K_2Ca_5(SO_4)_6.2H_2O$
Clastic mineral	
Quartz	SiO_2
Chlorite	$(Mg,Fe)_6(Si,Al)_4O_{10}(OH)_8$
Muscovite	$KAl_2Si_3AlO_{10}(OH)_2$
Montmorillonite	$Na_{0.3}(Al,Mg)_2Si_4O_{10}(OH)_2.H_2O$
Talc	$Mg_3Si_4O_{10}(OH)_2$
Pyrophyllite	$Al_2Si_4O_{10}(OH)_2$

Table 2. Mineralogy of depth facies of Mighan playa.

Facies	**Main mineral**	**Minor mineral**	**Trace mineral**
I	Gypsum, Quartz	Calcite, Basanite	Muscovite, Chlorite
II	Glauberite, Thenardite, Halite	Quartz	Magnesites, Gypsum
III	Gypsum, Basanite, Halite	Calcite, Quartz	Chlorite , Muscovite
IV	Halite, Gypsum	Basanite	Quartz, Talc, Chlorite, Muscovite

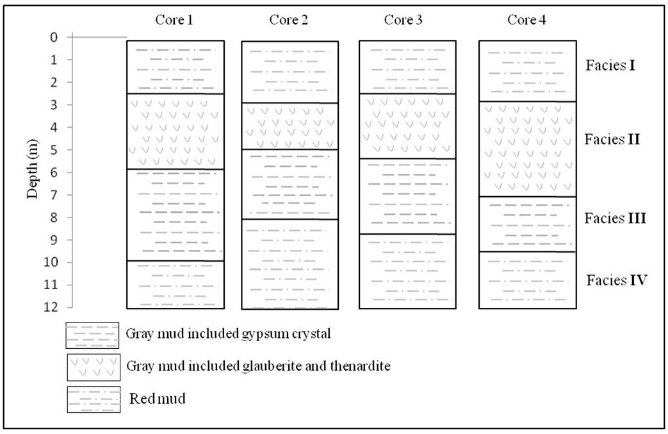

Fig. 2. Generalized lithological logs of the studied deposits from Mighan Lake.

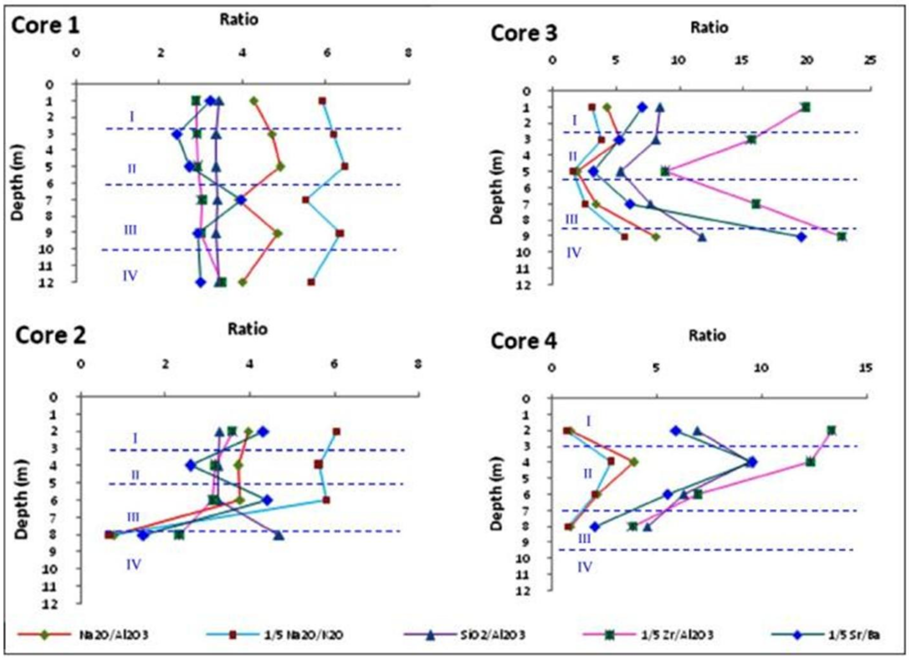

Fig. 3a. Variation of Na_2O/Al_2O_3, Na_2O/K_2O_3, SiO_2/Al_2O_3, Zr/Al_2O_3 and Sr/Ba in four cores of the Mighan playa.

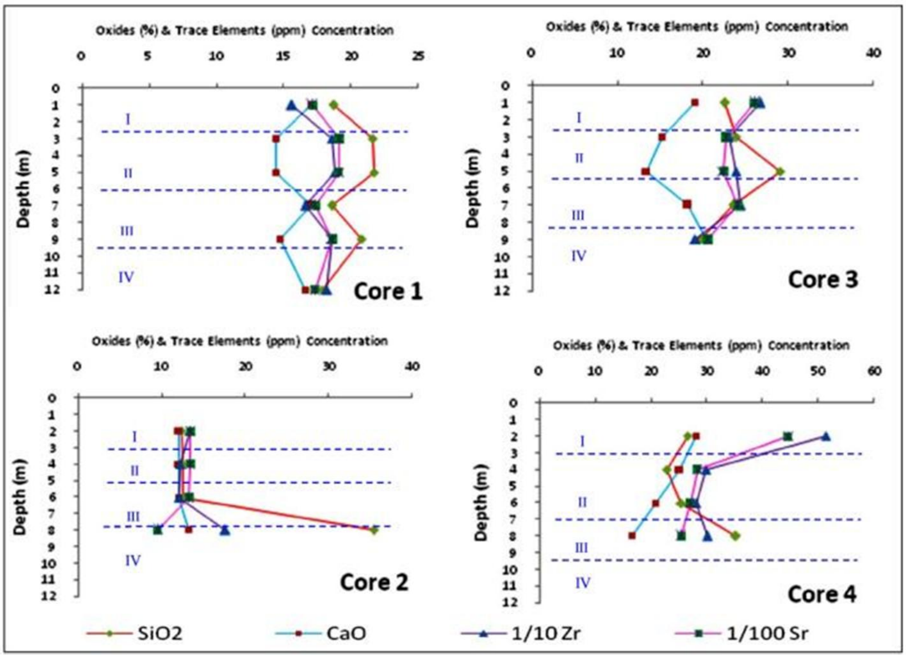

Fig. 3b. Variation of SiO_2, CaO, 1/10Zr and 1/100Sr in four cores of the Mighan playa.

7. Variables Relationships

In order to understand the inter-relationship between the major oxides and trace elements (4 variables) and 6 proxies obtained from 25 samples of the Mighan playa were standardized with the transformation function, Z= (X-M)/S (where X is the value of the variable, M is the mean and S is the standard deviation), to overcome, the non-Gaussian nature [14]. Factor analysis and cluster analysis were applied to identify sources of geochemical data in the sediments by applying aquamax normalized rotation. By extracting the eigenvalues from the correlation matrix, the number of significant factors explained by each of them was calculated [18]. Fig. 4 shows the results of the factor loading with aquamax normalized rotation. The results indicate that there were four source processes. For authorized factor analysis we applied cluster analysis. The hierarchical clustering by applying the complete linkage method was performed on the standardized data set. The cluster analyses for the geochemical data studied are shown in Fig. 5 as a dendogram. Fig. 5 displays four clusters; (1) SiO_2; (2) CaO-Sr-Zr; (3) Na_2O/K_2O-Na_2O/Al_2O_3; (4) Sr/Br-Zr/Al_2O_3-SiO_2/Al_2O_3.

8. Discussion

Both younger and older gray mud as well as older red mud are all interpreted as lake deposits that formed in ephemeral lakes. Evidence leading to this conclusion includes texture, sedimentary and pedogenic structures. The dominantly clay texture demonstrates that much of the sediment was deposited from suspended load in ponded water. Erosion of the upland by storm runoff supplied silt and clay that moved down as drainage [17]. When the mixed load encountered the lake, fine grains were transported out into the lake. Preserved fine lamination in muds demonstrated lake deposition. High organic content and dark colors are evidence of ponding and diminished oxidation. All modern and older muds have intensely developed soil structures. Sedimentary bedding is disrupted and homogenized by pedogenic processes. Roots, fractures and slickensided structures are evidence of soil formation. Silt admixed with clay may partly reflect incorporation of surface silt layers into the soil during dry periods. Precipitation of carbonate nodules and partial or complete oxidation of gray muds to red, suggests more intense or prolonged soil formation. Precipitation of pedogenic carbonate and formation of oxidized colors indicate an environment where less ponding occurred. Preservation of bedding in some red muds suggests that they may have been deposited with minimal soil formation but in environments that had a lesser amount of reducing or less organic rich depositional environments.

Several features of the deposits relate to the formation of the layered and unstratified intervals reflecting periods of shallow and greater depth of the lake [9]. The existence of this relationship between glauberite texture and water depth is mainly deduced from the nature of the textural features of the glauberite deposits. The laminated central parts of low glauberite content must have formed over periods of several years when, water concentrations of the lake were below the glauberite saturation. The preservation of a laminated structure is more directly related to periods with high lake levels and an absence of post-depositional physical disturbance or bioturbation. The absence of lamination in the lower and upper parts of these intervals is indicative of lower lake levels. The lake also had a higher salinity during these early and late stages.

The uniformity of the unstratified deposits reflects an absence of short-term variations in environmental conditions that are clearly recorded by the layered intervals. This lower sensitivity is related to brine composition which is less affected by an influx of freshwater or by changes in evaporation rates. The unstratified sections also do not have the typical textural features, indicative of shallow water depths. The large crystal size of the unstratified deposits indicates the absence of periods with a high degree of supersaturation.

The presence of muscovite (mica), quartz, chlorite, and talc in the sediments of the playa, points to metamorphic rocks as a source. These minerals are transported to the playa by fluvial processes from the surrounding mountains. Geological studies of the Mighan basin (Mighan playa is the center of this basin) indicate the presence of slate, phylite, metamorphosed sandstone and crystallized limestone [13]. The preservation of mica, chlorite and talc in the sediments of the playa indicates a relatively low degree of chemical weathering [15].

During the progressive evaporation of water in a saline lake, the sequence of minerals precipitated follow the chemical divides proposed by Eugster and Hardie [2, 3]. During evaporation, saturation with respect to alkaline earth carbonates is reached quickly. Therefore, calcite precipitates during the early stages of salinity increase. Subsequent precipitation of a mineral sequence of sulfates and chlorides is controlled by the relative concentration of Ca, Mg, HCO_3, SO_4 and Cl. Carbonate precipitation may also occur at higher salinities within the field of gypsum or halite precipitation [16]. This generally implies external influences such as aninflux of bicarbonate and Ca-rich brine through groundwater. The evaporite mineralogy of the sediment cores from the Mighan playa supports this model in a broad way.

Carbonates are the most widespread evaporites in the sediments occurring at all depths. Calcite and magnesite are the main carbonate minerals. In the cores, the sediment in units I and III have an evaporite assemblage of gypsum, basanite, calcite and halite.

This is in contrast with the sediments in unite II, where gypsum is conspicuously absent and the sulfate mineral assemblage is represented by glauberite and thenordite. This suggests a change in the brine evaporation chemistry corresponding to this depth. It is possible that during an early stage of lake evolution when deeper sediments were deposited, Ca concentrations in the brine were higher than the alkalinity on an equivalent basis (Ca>alkalinity). The brine therefore evolved depositing calcite and gypsum. Further evaporation under the conditions of alkalinity greater than Ca and Mg led to the precipitation of glauberite and thenardite in the sediment. The occurrence of glauberite can be attributed to different reasons. Glauberite is an authigenic mineral and it generally forms at the expense of gypsum deposited earlier due to a reaction with Na-rich brines [3].

For paleoclimatic interpretations, four shallow cores from different parts of the Mighan playa were taken into consideration. The geochemical unites (I-IV) mirror the different environments of deposition and possible pore water activity. As discussed earlier, the lower values of ratios Na_2O/Al_2O_3 and Na_2O/K_2O would indicate higher chemical weathering (humid climate) and vice versa. In a dominantly clastic environment, SiO_2/Al_2O_3 indicates the variation of quartz to feldspar ratio is actually terrigenous input, as neither of them are influenced by diagenetic processes. Zircon normally occurs in silt fraction and is transported with quartz grains by extrabasional processes [5]. As Sr is mainly present in carbonates, the Sr/Ba ratio is indicative of the variation of carbonate to detrital fractions. Higher values of the calculated ratio Na_2O/Al_2O_3, Na_2O/K_2O in unite II that corresponded to sodium-sulfate facies indicate higher aridity and low chemical weathering in the sedimentary history of the Mighan playa cores. This interpretation is supported by the higher concentration of SiO_2 and Zr in the sediments of unite II of the Mighan playa. The arid climate of the region is mirrored by the low chemical weathering and maximum aeolian input (SiO_2 and Zr) [19]. Unites I and III show the highest SiO_2/Al_2O_3, Zr/ Al_2O_3 and Sr/Ba ratio that corresponds to the highest degree of chemical weathering during this phase. Therefore, unite I and unite III represent a humid phase in the history of the Mighan playa sedimentation. The highest concentration of CaO and Sr indicate authigenic mineralization of gypsum and calcite in unites I and III.

Factor analysis and cluster analysis among the variables identified four main sources for geochemical unites that correspond to various facies.

1. SiO_2 represent extrabasional processes and possible eolian factor
2. CaO, Sr and Zr is mainly present as a factor in carbonates
3. Na_2O/K_2O, Na_2O/Al_2O_3 ratio is an indicator of aridity factor
4. SiO_2/Al_2O_3, Zr/Al_2O_3 and Sr/Ba ratios represent terrigenous factors due to fluvial processes

Table 3. Average concentration of major oxides and trace elements in the depth cores.

	Core1 (n=6)	Core2 (n=4)	Core3 (n=5)	Core4 (n=4)
Oxides (mass %)				
Na_2O	5.23	12.43	12.32	7.22
MgO	5.45	4.60	4.43	4.54
Al_2O_3	5.86	4.74	3.15	5.26
SiO_2	19.84	18.19	23.74	27.47
P_2O_5	0.08	0.07	0.06	0.07
CaO	15.70	12.43	17.26	22.60
K_2O	0.88	0.80	0.84	1.07
TiO_2	0.36	0.30	0.13	0.18
MnO	0.07	0.05	0.03	0.04
Fe_2O_3	3.40	2.84	1.57	2.25
Trace element (mg/kg)				
Cu	4.00	1.25	4	2.02
Zn	57.17	41.00	70.80	91.50
Rb	38.83	33	29.80	43.75
Sr	1811	1236	2316	3125
Zr	88.67	69	234	348
Ba	122.83	82.50	80.00	138

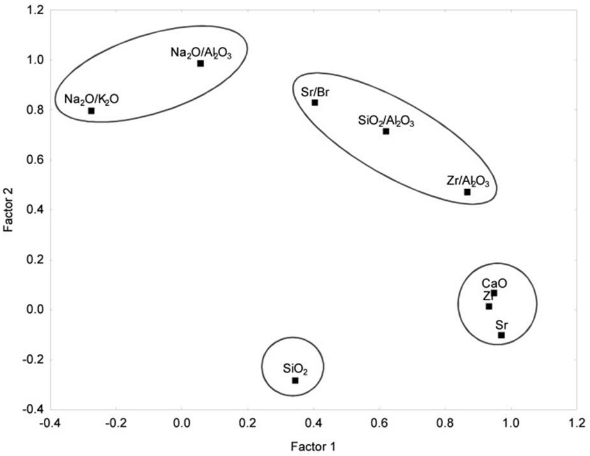

Fig. 4. Factor analysis results in two dimensional Space: plot of loading of the first and second factor.

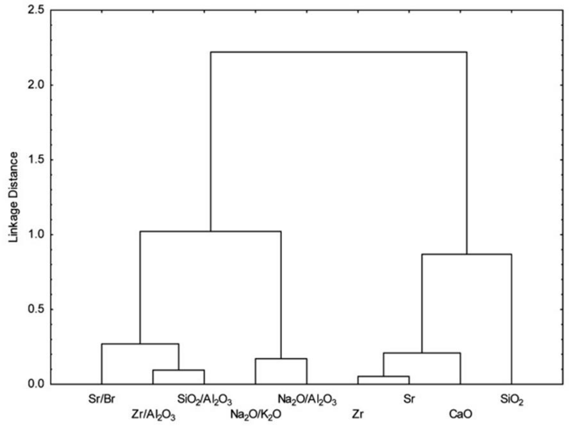

Fig. 5. Dendogram results using Ward‘s Method of Hierarchical Cluster Analysis for variables.

9. Conclusion

The Mighan playa accumulated heterogeneous sediments through much of the Holocene. Climatic fluctuations are documented by vertical heterogeneities resulting from changes in sediment supply, lake expansion, and type of sediment.

1. Gypsum and calcite are the main sulfates and carbonates above and below the studied depth. It is absent in the middle depth where glauberite, thenardite and halite represent the sulfate component. This indicates a sharp change in brine chemistry.
2. Applying the mineralogical data to the Eugster and Hardie evaporation model, it is inferred that during the early stages of the evolution of the Mighan playa, Ca concentrations in the brine were higher than alkalinity which favored the precipitation of gypsum. During a more recent evaporation path, an alkalinity greater than Ca concentrations created an assemblage of sulfate and chlorides (glauberite, halite and thenardite). The overall brine chemistry therefore changed from Ca-Mg-SO_4-Cl to Na-SO_4-Cl type.
3. The detrital materials in the playa sediments are derived from the metamorphic rocks of the Arak Mountains.
4. The geochemical proxies, e.g, Na_2O/Al_2O_3, Na_2O/K_2O, SiO_2/Al_2O_3, Zr/Al_2O_3, Sr/Ba and mineralogical data enabled us to separate the shallow cores into three different environments of deposition. The arid (sub-) unite (II) is characterized by the presence of evaporites (glauberite, thenardite and halite) and a high Na_2O/Al_2O_3 and Na_2O/K_2O ratio. The SiO_2/ Al_2O_3 and Zr/Al_2O_3 ratio indicates relatively terrigenous material from the extrabasin to the Mighan playa by rivers as well as indications of chemical weathering in unites I and III.

Acknowledgments

This research was supported by the Mining and Industrial Organization of Markazi Province. I wish to thank them for their cooperation in the field work and for sample collection and preparation.

References

[1] Emami, S., 1991. Geological Map of Qom. Geology Survey of Iran, in Farsi.

[2] Eugster, H.P., Hardie, L.A., 1978. Saline lakes. In; Lermon, A. (Ed.), Lakes; Chemistry, Geology, Physics. Springer-Verlage, pp. 237-293.

[3] Hardie, L.A., 1968. The origin of the recent non-marine evaporite deposit of Saline Valley, Ingo County, California. Geochim. Cosmochim. Acta 32 (1279-1301).

[4] Harrington, N.M., Herczeg, A.L., Salle, C., 2008. Hydrological and geochemical processes controlling variation in Na^+-Mg^{2+}-Cl^--SO_4^{2-} groundwater brines, south-eastern Australia, Chemical Geology 251, 8-19.

[5] Haug, G.H., Gunther, D., Peterson, L.C., Sigman, D.M., Highen, K.A., Aeschlimann, B., 2003. Climate and the collapse of Maya Civilization, Science 299, 1731-1735.

[6] Huerta, P., Armenteros, I., Recio, C., Blanco, A.J., 2010. Palaogroundwater evolution in playa-lake environments. Sedimentary facies and stable isotope record. Palaeography, palaeoclimatology,Palaeoecology 286, 135-148.

[7] Last, W.M., Vance, R.E., 2002. The Holocene history of Oro Lake, one of the western Canada's longest continuous lacustrine records. Sediment. Geol. 148, 161-184.

[8] Li, M., Fang, X., Yi, C., Gao, S., Zhang, W., Galy, A., 2010. Evaporite minerals and geochemistry of the upper 400 m sediments in a core from the western Qaidam Basin, Tibet, Quaternary International 218, 176-189.

[9] Mees, F., 1999. Textural features of Holocene perennial saline lake deposits of the Taoundenni–Agorgott Basin, northern Mali, Sedimentary Geology 127, pp 65-84.

[10] Mees, F., Castaneda, C., Herrer, J., Ranst, V.E., 2011. Bloedite sedimentation in a seasonally dry saline lake (Salada Mediana, Spain). Sedimantary Geology 238, 106-115.

[11] Mohajarani, S., 1999. Determination Mighan sediments province, Ms. Thesis in Tehran University, In Farsi.

[12] Ori, G.T., 2010. The sedimentary record of modern and ancient dray lake. Lakes on Mars: 10. 1016.

[13] Pedrami, M., 1988. Quaternary geology and climatology of Arak area. Internal report of the Geological Survey of Iran, 3-11.

[14] Ramhumar, M., Berner, Z., Stuben, D., 2002. Multivariate statistical discrimination of selected carbonate petrographic classification: Implications on applicability of classified systems and predictability of petrographic types. Chemic der Erde (Geochemistry) 62, 145-159.

[15] Roy, P.P., Smykatz-kloss, W., Sinha, R., 2006. Late Holocene geochemical history inferred from Sambhar and Didwana playa sediments,Thar desert, India: Comparison and synthesis. Quaternary International 144, 84-98.

[16] Schreiber, B.C., 1998. Sedimentary and diagenetic transitions between carbonates and evaporites. 15th International Sedimentological Congress, Alicante, PP. 704-705.

[17] Simpkins, W.W., Gustavson, T.C., Finley, R, J., 1982. Erosion process studies in the Texas Panhandle–analysis of a 2-year data record: The University of Texas at Austing, Bureau of Economic Geology Geological Circular82-7: 168-175.

[18] Subborao, C., Subbarao, N.V., Chandu, S.N., 1995. Characterization of groundwater contamination using factor analysis. Environmental Geology 28, 175-180.

[19] Tripathi, J.K., Rajamani, V., 1999. Geochemistry of the loessic sediments on Dehli ridge, eastern Thar Desert, Rajastan: impilication for exogenic processes, Chemical Geology 155, 265-278.

[20] Veigas, J.G., Rosell, L., Orti, F., Gundogan, T., Helvaci, C., 2011. Mineralogy, diagenesis and hydrochemical evolution in a probertit-glauberite-halite saline lake (Miocene, Emet Basin, Turkey), Chemical Geology 280, 35-364.

[21] Zamani, F., 1999. Sedimentology Arak Mighan Lake. Ms. Thesis in Beheshti University, In: Farsi.